

Organic transistors and circuits with parylene gate dielectric manufactured using subfemtoliter inkjet

Tomoyuki Yokota¹, Yoshiaki Noguchi¹, Yusaku Kato¹, Tsuyoshi Sekitani², and Takao Someya^{1,2,3}

¹Applied Physics, University of Tokyo,

7-3-1 Hongo, Bunkyo, Tokyo 113-8656, Japan

Phone: +81-3-5841-6756 E-mail: yokota@ntech.t.u-tokyo.ac.jp

²Electrical and Electronic Engineering and Information Systems, University of Tokyo,

7-3-1 Hongo, Bunkyo, Tokyo 113-8656, Japan

³Institute for Nano Quantum Information Electronics (INQIE), University of Tokyo,

7-3-1 Hongo, Bunkyo, Tokyo 113-8656, Japan

1. Introduction

Organic electronics have attracted much attention for their in low cost, large area process, light weight, mechanical flexibility, and low-temperature processing. Particularly, organic thin-film transistors (TFTs) are expected to be key parts which realize organic mechanically flexible electronics, for example e-paper [1], flexible RFID tags [2], large-area sensors [3, 4], and digital circuits.

As highly efficient methods to manufacture organic TFTs, printing technology such as inkjet printing [5], micro-contact printing [6], and screen printing [7], have attracted much attention. However, the resolution of the normal inkjet process is about 40~50 μm because it is difficult to reduce the droplet volume below 1 pl.

In this work, we fabricated organic TFTs with top contact geometry by subfemtoliter inkjet printing technology and integrated the organic TFTs into organic complementary (CMOS) ring oscillator circuits. The TFTs have a channel length smaller than 10 μm , a channel width 500 μm , and the 3 μm -linewidth Ag source/drain electrodes. The mobility is 0.1 cm^2/Vs and the on/off current ratio is 10^7 .

2. Fabrication process

The cross-sectional illustration of the organic transistor is shown in Figure 1(a). These transistors are fabricated by vacuum evaporation and inkjet printing processes. First, a 30-nm-thick Au layer is thermally evaporated on a polyimide substrate through a shadow mask to form gate electrode. Then, a parylene film was covered on the gate electrodes by chemical vapor deposition to form an insulating layer, whose thickness was 60 nm or 260 nm. On the parylene layers, 50-nm-thick pentacene film or 30-nm-thick F_{16}CuPc was fabricated by thermal evaporation as a p-type or n-type organic semiconductor channels. Following the deposition, a 50-nm-thick Au pad was sublimated by vacuum evaporation with a shadow mask. Finally, Ag lines were patterned by subfemtoliter inkjet systems and were sintered at 100 $^\circ\text{C}$ for 3 hours in nitrogen environment to form source and drain electrodes. Fig.1(b) shows a photograph of the fabricated devices. The TFTs have a channel length of 3 μm , a channel width of 500 μm , and the 3 μm -linewidth Ag source/drain electrodes.

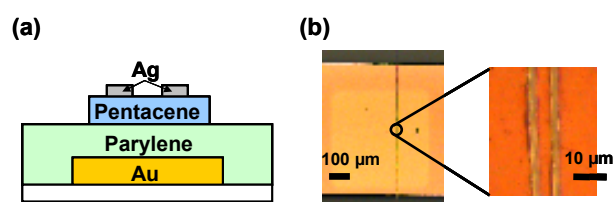


Fig. 1 (a)The cross-sectional illustration of the organic transistor. (b)The optical microscope image of organic FET with channel length of 3 μm .

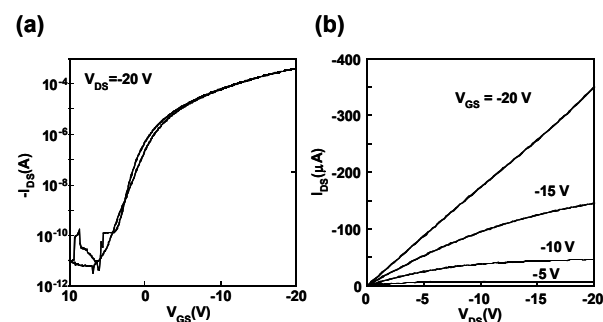


Fig. 2 Transistor characteristics of the pentacene TFTs with channel length of 3 μm and channel width of 500 μm . (a)Transfer characteristics (b)Output characteristics

3. Results

Fig. 2 shows electric properties of fabricated organic transistor with channel length and width of 3 μm , 500 μm respectively. The mobility is 0.1 cm^2/Vs and on/off current ratio is 10^7 .

Then, we measured electric properties of fabricated organic transistors. When the channel length is changed from 97 μm to 6 μm , the transfer curves systematically shift from right to left along the horizontal axis, or to the positive V_{GS} , as shown in figure 3 (a). Fig.3 (b) shows output characteristics of organic transistor with channel length of 6 μm and channel width of 500 μm . This shift may be due to the short channel effect. The dependence of the mobilities and threshold voltages of the transistors on channel length is shown in figure 4 (a) and (b).

Next, we measured the characteristics of 3-stage organic CMOS ring oscillator. Fig.5 (a) shows photograph of the CMOS ring oscillator. The mobilities of pentacene and

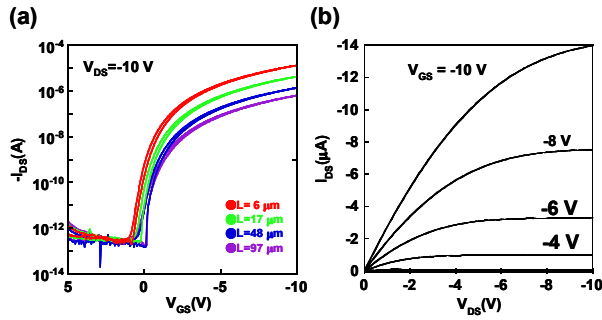


Fig. 3 Transistor characteristics of the pentacene FETs (a) Transfer characteristics of pentacene TFTs with channel length of 6 μm , 17 μm , 47 μm , and 97 μm (channel width is 500 μm for all devices). (b) Output characteristics of pentacene TFTs with channel length of 6 μm and channel width of 500 μm .

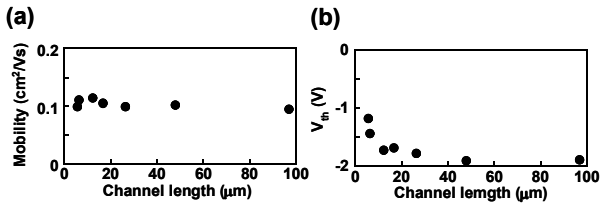


Fig. 4 (a) Mobility (b) threshold voltage (V_{th}) of pentacene TFTs with channel length of 6 μm to 97 μm .

$F_{16}\text{CuPc}$ TFTs that make up the ring oscillators are 0.22 and 0.007 cm^2/Vs , respectively. The channel widths and the channel lengths of the p-type transistors are 526 μm and 43 μm , respectively. The channel widths and the channel lengths of the n-type transistors are 4092 μm and 8.7 μm , respectively. Input-output characteristics of organic CMOS inverters are shown in Figure 5(b), demonstrating excellent characteristics of CMOS inverter. The organic integrated circuits oscillated at 2.26 kHz when the drain voltage (V_{DD}) was 40 V (Fig.5(c)). We have measured V_{DD} dependence of oscillating frequency of the organic CMOS oscillators (Fig.5(d)). This oscillator can be operated even at 5 V.

3. Conclusions

We have manufactured high performance organic TFTs with top-contact geometry and organic CMOS ring oscillators with inkjet systems which control subfemtoliter ink droplets and measured the electric characteristics and observed the oscillation of the devices. From this experiment, we showed the line widths of source and drain electrodes of the organic TFTs have an influence on the frequency response of the transistors and its circuits. These results demonstrate that the miniaturization of electrodes of organic TFTs are effective for realizing high speed operation organic devices.

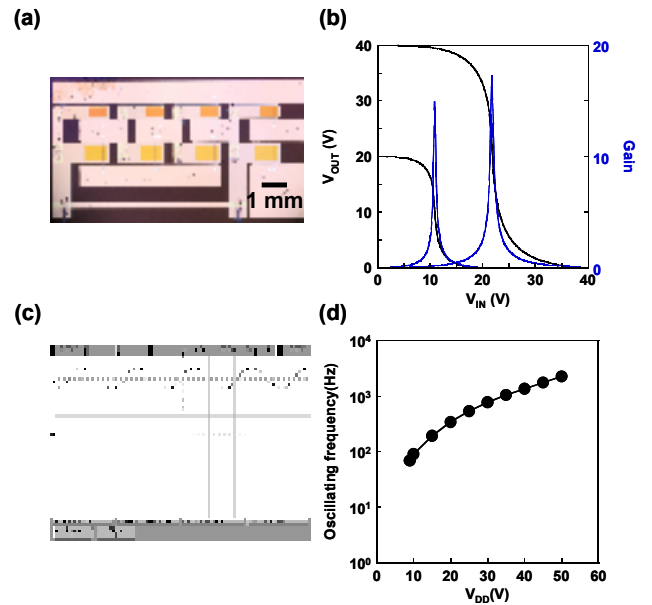


Fig. 5 (a) Micrograph of the organic CMOS ring oscillator with inkjet printed source and drain electrodes. (b) Input-output characteristics of organic CMOS inverters in fabricated ring oscillators. (c) Output signals at a V_{DD} of 40 V of integrated 3-stage CMOS ring oscillator with printed source and drain electrodes. The oscillation frequency of the oscillator at this voltage is 2.26 kHz. (d) Oscillating frequency of fabricated ring oscillators as a function of V_{DD} .

4. Acknowledgements

We thank Harima Chemicals for providing high-quality Ag nanoparticles, and SIJ Technology for technical support in the inkjet process. This work is partially supported by Special Coordination Funds for Promoting, JST/CREST and KAKENHI (Wakate S). One of the authors (T.Y.) is grateful to the research fellowships for young scientists of JSPS.

5. References

- [1] J. A. Rogers, Z. Bao, K. Baldwin, A. Dodabalapur, B. Crone, V. R. Raju, V. Kuck, H. Katz, K. Amundson, J. Ewing, and P. Drzagic, Proc. Natl. Acad. U.S.A. **98**, 4835 (2001).
- [2] P. F. Baude, D. A. Ender, M. A. Haase, T. W. Kelley, D. V. Muryes, and S. D. Theiss, Appl. Phys. Lett. **82**, 3964 (2003).
- [3] T. Someya, T. Sekitani, S. Iba, Y. Kato, H. Kawaguchi, and T. Sakurai, Proc. Natl. Acad. U.S.A. **101**, 9966 (2004).
- [4] T. Someya, Y. Kato, T. Sekitani, S. Iba, Y. Noguchi, Y. Murase, H. Kawaguchi, and T. Sakurai, Proc. Natl. Acad. U.S.A. **102**, 12321 (2005).
- [5] T. Kawase, S. Moriya, C. J. Newsome, and T. Shimoda, Jpn. J. Appl. Phys. **44**, 3649 (2005).
- [6] M. Leufgen, A. Lebib, T. Muck, U. Bass, V. Wagner, T. Borzenko, G. Schmidt, J. Geurts, and L. W. Molenkamp, Appl. Phys. Lett. **84**, 1582 (2004).
- [7] Y. Noguchi, T. Sekitani, and T. Someya, Appl. Phys. Lett. **91**, 133502 (2007).